



**HAL**  
open science

## Effects of some ion-specific properties in the electrocoagulation process with aluminum electrodes

Jean-Luc Trompette, Jean-Francois Lahitte

► **To cite this version:**

Jean-Luc Trompette, Jean-Francois Lahitte. Effects of some ion-specific properties in the electrocoagulation process with aluminum electrodes. *Colloids and Surfaces A: Physicochemical and Engineering Aspects*, 2021, 629, pp.127507. 10.1016/j.colsurfa.2021.127507 . hal-03342993

**HAL Id: hal-03342993**

**<https://hal.science/hal-03342993>**

Submitted on 16 Sep 2021

**HAL** is a multi-disciplinary open access archive for the deposit and dissemination of scientific research documents, whether they are published or not. The documents may come from teaching and research institutions in France or abroad, or from public or private research centers.

L'archive ouverte pluridisciplinaire **HAL**, est destinée au dépôt et à la diffusion de documents scientifiques de niveau recherche, publiés ou non, émanant des établissements d'enseignement et de recherche français ou étrangers, des laboratoires publics ou privés.



[Open Archive Toulouse Archive Ouverte](#)

OATAO is an open access repository that collects the work of Toulouse researchers and makes it freely available over the web where possible

This is an author's version published in: <http://oatao.univ-toulouse.fr/28281>

Official URL : <https://doi.org/10.1016/j.colsurfa.2021.127507>

**To cite this version:**

Trompette, Jean-Luc  and Lahitte, Jean-François  *Effects of some ion-specific properties in the electrocoagulation process with aluminum electrodes.* (2021) *Colloids and Surfaces A: Physicochemical and Engineering Aspects*, 629. 127507. ISSN 0927-7757

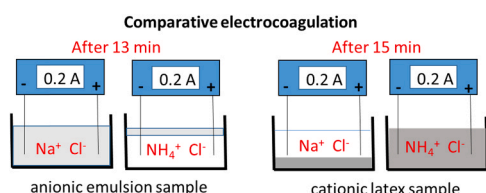
Any correspondence concerning this service should be sent to the repository administrator: [tech-oatao@listes-diff.inp-toulouse.fr](mailto:tech-oatao@listes-diff.inp-toulouse.fr)

# Effects of some ion-specific properties in the electrocoagulation process with aluminum electrodes

Jean-Luc Trompette<sup>a,\*</sup>, Jean-François Lahitte<sup>a</sup>

<sup>a</sup> Laboratoire de Génie Chimique UMR 5503, Université de Toulouse, CNRS, 4 Allée Emile Monso, 31432 Toulouse Cedex 4, France

## GRAPHICAL ABSTRACT



## ARTICLE INFO

**Keywords:**  
Electrocoagulation  
Ionic-specificity  
Faradaic efficiency  
pH effects

## ABSTRACT

The influence of anion specificity on the faradaic efficiency relative to aluminum oxidation during electrocoagulation has been reported. While with chaotrope anions, the faradaic efficiency is higher than 1, it is lower than 1 with kosmotrope anions. The origin of this distinction has been ascribed to the ability of anions to cause pitting through the thin passive film at the aluminum surface, which depends on the varying resistance of the anions to dehydration. The influence of the nature of the cation of the supporting electrolyte on the efficiency of electrocoagulation has been investigated by comparing the same treatment of two characteristic colloidal samples. While removal efficiency is better for a positively charged latex in the presence of sodium chloride, it is better for a negatively charged oil in water emulsion in the presence of ammonium chloride. The results come from different effects of pH and its influence on aluminum species during electrocoagulation.

## 1. Introduction

Numerous studies have been devoted to the treatment of fluids of different nature through the electrocoagulation process with aluminum plates as sacrificial electrodes. General reviews have compiled the main conclusions as well as the expectations of this technology [1–6]. Owing to its convenience, cheapness and safety, this electrochemical technique attracts continued attention due to the growing constraint of environmental considerations. This is particularly the case in the context of global warming because the reuse and valorization of wastewater is an important topic. In this sense, the use of microbial fuel cell as a

self-powered electrolyzer for electrocoagulation of diverse effluents is representative and promising [7,8].

Moreover, the rejection of wastewaters polluted by plastic polymers is a serious environmental challenge since the generated micro- and nanoplastics may enter the food chain, resulting in exposure of consumers. Indeed, as most plastics start to degrade at their polymer surface, through machining or weathering and aging, smaller fragments are formed which in turn have a higher fragmentation rate due to their increasingly higher surface-to-volume ratio. These erosion processes promote the appearance of electric charges on the surface of fragments of the same nature, so allowing them to remain dispersed in aqueous

\* Corresponding author.

E-mail address: [jeanluc.trompette@toulouse-inp.fr](mailto:jeanluc.trompette@toulouse-inp.fr) (J.-L. Trompette).

<https://doi.org/10.1016/j.colsurfa.2021.127507>

Received 11 May 2021; Received in revised form 2 September 2021; Accepted 2 September 2021

Available online 4 September 2021

0927-7757/

effluents. The resulting nanoplastics thus present the same characteristics as lyophobic charged nanoparticles. Although electrocoagulation is a suitable technique to remove such colloidal entities from aqueous media, it has been devoted in a huge majority with the treatment of negatively charged samples (nanoparticles or drops) but studies concerning cationic entities are very scarce (the removal of heavy metal cations is not considered as it refers to ions). This is not surprising since the isoelectric point (iep) of colloidal entities, from natural or synthetic origin, is very often lower than the usual initial pH, between 6 and 7, where electrocoagulation experiments are performed. Owing to diverse origins of nanoplastics rejected in wastewaters with different properties (pH, salinity, ionic detergents) there is a need to achieve a better knowledge of conditions allowing an optimal removal through electrocoagulation whatever the surface charge.

In earlier studies, the influence of sodium and ammonium electrolytes on the efficiency of the electrocoagulation process to treat various negatively charged samples (polymer latex, emulsion) with aluminum electrodes has been reported [9,10]. Since the stability of colloidal systems is dominated by electrostatic effects, i.e. long-range interactions, the different nature of dispersed entities has not a real influence on electrocoagulation treatments. By avoiding an excessive increase of solution pH in the presence of ammonium ions through a buffer effect, formation of aluminate anions was disadvantaged so that the proportion of efficient coagulating aluminum species was promoted. As a result, the separation kinetics of the previous studied systems was more effective and shorter (reduced electrical consumption) with ammonium salt. However, it is questionable whether the same would be true with positively charged particles since aluminate counterions should not be favored when using ammonium salt.

In addition, although the general principles of electrocoagulation are known, there remain some controversial aspects at the fundamental level. It is for instance the case of super-faradaic efficiency. It is often estimated in electrocoagulation studies, even in the presence of complex fluids, since the coagulant dose is an important parameter of this process [11–13]. However, it has to be noted that faradaic efficiency was estimated only in the presence of chloride salts in previous studies.

In the first part of this study, the influence of anion specificity on the faradaic efficiency has been investigated by using selected sodium electrolytes. In the second part, the same electrocoagulation treatment has been applied to a negatively charged oil in water emulsion and a positively charged polymer latex in the presence of NaCl and NH<sub>4</sub>Cl electrolytes at 0.01 mol/L concentration to compare the results according to the nature of the cation. All electrolysis experiments were conducted by imposing a constant 0.200 A electrical intensity.

## 2. Material and methods

### 2.1. Materials

Small aluminum plates were cut from a commercial sheet of 1050 aluminum sample (chemical composition in per cent weight: 99.5% Al, <0.40% Fe, <0.25% Si, <0.05% Cu) to obtain a rectangular shape, i.e. 3 cm × 1 cm × 0.05 cm. Prior to each experiment, the aluminum plates were abraded with emery paper, degreased with acetone, rinsed with water and dried in air.

Sodium chloride (NaCl), sodium perchlorate (NaClO<sub>4</sub>), sodium thiocyanate (NaSCN), sodium sulfate (Na<sub>2</sub>SO<sub>4</sub>), sodium bromide (NaBr), sodium fluoride (NaF), sodium acetate (NaC<sub>2</sub>H<sub>3</sub>O<sub>2</sub>), sodium iodate (NaIO<sub>3</sub>), sodium nitrate (NaNO<sub>3</sub>), sodium dihydrogen phosphate (NaH<sub>2</sub>PO<sub>4</sub>) and ammonium chloride (NH<sub>4</sub>Cl) were purchased by Sigma-Aldrich or Prolabo and were used as received. Deionized water was taken as a solvent to prepare 100 mL of electrolytic solutions at 0.01 mol/L concentration.

Semi-skimmed bovine milk (Lactel) was used as a representative stable oil in water emulsion. A sample of 4 mL of semi-skimmed milk was diluted with water to obtain 100 mL of solution with a 0.01 mol/L

NaCl or NH<sub>4</sub>Cl electrolyte concentration. The measured pH was 7.0, the conductivity at 25 °C was 2.0 and 1.7 mS/cm, respectively, with ammonium and sodium chloride.

Stable polystyrene latex was synthesized from surfactant-free emulsion polymerization according to classical methods reported in the literature [14,15]. Nitrogen gas was bubbled during 10 min into 100 mL of deionized water containing 0.023 g of 2,2'-azobis(2-methylpropionamide) dihydrochloride initiator (AIBA, 271.19 g/mol) from Acros Organics (98%). The solution was placed into a double-jacketed reactor at 70 °C using a regulating bath (Lauda EcoSilver) and it was moderately agitated (250 rpm) with a magnetic stirrer. The inhibitor present in liquid styrene was removed by filtration across a bed of activated alumina powder. Then, 1 mL of purified styrene (C<sub>8</sub>H<sub>8</sub>, 104.15 g/mol, density: 0.906 g/mL) was added into the previous solution and reaction was stopped after 8 h. After synthesis, 30 mL of the obtained latex was poured in a dialysis bag (12–14 kDa, regenerated cellulose). It was then immersed in 1.8 L of deionized water under gentle agitation. The conductivity of the contact water was checked over time, and deionized water was changed until the conductivity of contact water reached 1 μS/cm. The conductivity, pH value, and dry content of the dialyzed latex sample were, respectively, 7 μS/cm, pH 6.3, and 0.76%.

### 2.2. Electrochemical device

The experiments were carried out with two parallel electrode plates. An aluminum plate as the anode and a platinum plate as the cathode were used for experiments in Section 3.1, and two aluminum plates were used for experiments in Section 3.2. The distance between the electrodes was fixed at 2.5 cm and the electrodes were immersed at 2 cm depth in 100 mL of electrolytic solution. The active geometric area of the anode is 4.25 cm<sup>2</sup>, i.e. 2 × (2 cm × 1 cm) for the faces + 2 × (2 cm × 0.05 cm) for the lateral sides + 1 cm × 0.05 cm for the bottom side. All electrolysis experiments were performed by imposing a 0.200 A electrical intensity through a DC power supply (Convergie Fontaine, 1 A - 400 V). The electrical intensity was checked to be constant during experiments with the use of an amperemeter. Solutions were gently agitated with a magnetic stirrer. All electrocoagulation experiments were repeated twice.

### 2.3. Analysis methods

The aluminum content in aqueous solution was measured by inductively coupled plasma emission spectroscopy (ICP-OES, Horiba Jobin Yvon - Ultima 2). After the electrolysis experiments, the samples were immediately acidified with nitric acid (HNO<sub>3</sub>) to dissolve completely aluminum hydroxide precipitates.

The COD levels were determined using the standardized colorimetric technique (Hach) with an excess of chromium trioxide in sulfuric acid in glass vials and subsequent measurement of the optical density at 605 nm, the results were expressed as % COD removal.

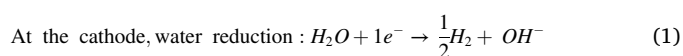
A Malvern NanoZS model was used for size and zeta potential measurements. Scanning electron microscopy (SEM) images were taken with a JEOL JSM 7100 F model operating at 10 kV.

An electronic pH-meter (Eutech Instruments) was used for the measurements.

## 3. Results and discussion

### 3.1. Influence of anion specificity on the faradaic efficiency

During electrocoagulation with a pair of aluminum electrodes, the following basic electrolytic reactions take place:

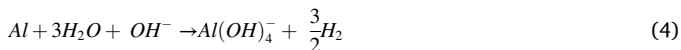


At the anode, aluminum oxidation :  $Al \rightarrow Al^{3+} + 3e^{-}$  (2)

and water oxidation :  $H_2O \rightarrow 2H^{+} + \frac{1}{2}O_2 + 2e^{-}$  (3)

although (2) is by far the major reaction at this electrode.

At the cathode where reaction (1) occurs, aluminum is chemically dissolved into aluminate anion owing to the alkaline environment in its vicinity:



The weight loss of aluminum cathode has been proven [16,17], the presence of a characteristic whitish veil on the cathode surface is often observed.

As aluminum plate undergoes oxidation reaction (2), the amount of released aluminum is often compared in electrocoagulation studies to that expected from the Faraday's law because the dosage of the coagulant is an important parameter for optimization of this process. A recognized advantage of this technology is to finely adjust the dose of coagulant in the system while aluminum salts or polyelectrolytes must be added during the chemical dosing technique [18,19]. When a constant electrical intensity  $i$  (A) is imposed, the theoretical amount  $m_{th}$  (g) of released aluminum may be controlled by varying electrolysis duration  $t$  (s) according to:

$$m_{th} = \frac{i \cdot t \cdot M_{Al}}{z \cdot F} \quad (5)$$

where  $M_{Al}$  is the atomic weight of aluminum (26.98 g/mol),  $z$  is the number of charges ( $z = 3$ ),  $F$  is the Faraday's constant (96,500 C/mol).

Chemical dissolution of aluminum plate, owing to the local acidity in the anode vicinity from reaction (3), was found to be insignificant [20].

The experimental amount of aluminum,  $m_{exp}$ , can be assessed from two main analysis: the weight loss of aluminum anode and/or the dosing of aluminum content in aqueous phase through ICP measurements. The faradaic efficiency corresponds to the ratio:

$$\Phi = \frac{m_{exp}}{m_{th}} \quad (6)$$

In the presence of a usual electrolyte like NaCl, the  $\Phi$  value has been found to be very often higher than 1 [17,20–24], except in a sole study where it was estimated to be not the case [25]. However, the origin of this super-faradaic efficiency remains an open debate. Whereas chloride anions have been assumed to catalyze pitting corrosion of aluminum [22,26,27], an intergranular corrosion mechanism has been postulated

during the dissolution of aluminum, so that aluminum grains were lost from the anode [24]. It has been reported that chemical dissolution of surface metal atoms with water molecules might occur in parallel to electrochemical corrosion to explain the findings [28]. Although it may be the case in quite acidic media, this is less likely in neutral aqueous solution. It has been proposed that super-faradaic charge yields for aluminum dissolution originate from the use of net currents in calculations instead of partial dissolution currents that should be used. The reason has been ascribed to a localized evolution of hydrogen in dissolution pits [20], although the exact cause remains unclear.

As in the case with other studies [17,23–25], the faradaic efficiency has been investigated in the presence of aqueous electrolyte solutions without colloidal entities to avoid any influence on the results, however selected electrolytes were tested. A platinum plate (inert material) was used as a cathode in electrolysis to ensure the anode was the sole source of aluminum during application of the same 0.200 A electrical intensity at different durations. The results obtained from the weight loss method and the ICP dosing method are reported in Fig. 1 in the case of NaCl. The replicability of this experiment is shown in Fig. S1 in Supporting Information. The results obtained in the same conditions with  $NaNO_3$ ,  $NaClO_4$ ,  $NaBr$  and  $NaSCN$  electrolytes have been reported in Supporting Information, respectively, in Figs. S2, S3, S4.

Whatever the electrolyte, the amount of aluminum from the loss weight method (open circle) is slightly greater or practically super-imposed with that of the dosing ICP method (open square), and both are greater than that predicted from the Faraday's law corresponding to the continuous line with slope 0.00112 g/min given by Eq. (5). This indicates that the faradaic efficiency is found to be higher than 1 whatever the method. With both methods, the weight of aluminum increases linearly as a function of electrolysis duration. Regression  $r^2$  values are very close to 1 so indicating the reliability of the measurements. The compared measurements in Fig. 1 with those in Fig. S1 confirm the repeatability of the results. The respective slopes (dashed line for loss weight method and dotted line for dosing method) allows calculating the representative faradaic efficiency by dividing this slope to that of the Faraday's law (0.00112 g/min) to give  $\Phi_w$  for the weight loss method and  $\Phi_d$  for the dosing method. All the corresponding values of the faradaic efficiency have been reported in Table 1.

As it can be seen in Table 1, the faradaic efficiency is higher than 1 whatever these electrolytes. The faradaic efficiency is highest with nitrate ( $NO_3^{-}$ ) anions whatever the method. After electrolysis, the aluminum anode exhibited the characteristic presence of corrosion pits on the surface with all these salts. A representative SEM image in the case of NaSCN electrolyte is shown in Fig. S5 in Supporting Information.

In the case of  $Na_2SO_4$ , NaF,  $NaH_2PO_4$ ,  $NaIO_3$  and  $NaCH_3CO_2$ , the

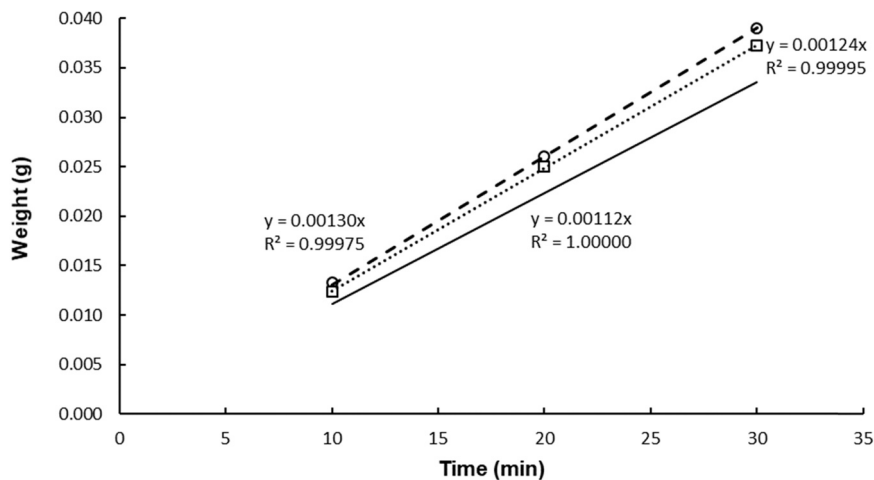


Fig. 1. Weight of aluminum from the loss weight method (○, dashed line) and from the ICP dosing method (□, dotted line) as a function of electrolysis duration in the presence of NaCl at 0.01 mol/L (the continuous line represents Faraday's law).

**Table 1**

Value of the faradaic efficiency from the weight loss method ( $\Phi_w$ ) and from the ICP dosing method ( $\Phi_d$ ) of the investigated electrolyte, and corresponding  $B$  value of the anion.

| Salt                              | $\Phi_w$ | $\Phi_d$                      | $B_{anion}$ (L/mol) |
|-----------------------------------|----------|-------------------------------|---------------------|
| NaCl                              | 1.16     | 1.11                          | -0.007              |
| NaNO <sub>3</sub>                 | 1.22     | 1.20                          | -0.046              |
| NaClO <sub>4</sub>                | 1.12     | 1.09                          | -0.061              |
| NaBr                              | 1.16     |                               | -0.032              |
| NaSCN                             | 1.08     |                               | -0.103              |
| Na <sub>2</sub> SO <sub>4</sub>   |          | 10': 0.36/20': 0.45/30': 0.63 | 0.208               |
| NaF                               |          | 5': 0.63/10': 0.55/20': 0.60  | 0.1                 |
| NaIO <sub>3</sub>                 |          | 5': 0.09/10': 0.13/15': 0.10  | 0.138               |
| NaH <sub>2</sub> PO <sub>4</sub>  |          | 10': 0.39                     | 0.34                |
| NaCH <sub>3</sub> CO <sub>2</sub> |          | 10': 0.42                     | 0.25                |

weight loss method could not be applied since after electrolysis the weight of the plate was often greater than initially, so reflecting that a hard precipitate with NaF (probably cryolite Na<sub>3</sub>AlF<sub>6</sub>) and NaCH<sub>3</sub>CO<sub>2</sub>, or an iridescent anodized film with Na<sub>2</sub>SO<sub>4</sub>, NaIO<sub>3</sub> and NaH<sub>2</sub>PO<sub>4</sub>, has been formed on the surface. Nevertheless the presence in solution of aluminum hydroxide precipitates, i.e. Al(OH)<sub>3</sub>, was obvious, so confirming the release of aluminum cations from the anode. However, as reported in Fig. 2 with the representative cases of NaF, Na<sub>2</sub>SO<sub>4</sub> and NaIO<sub>3</sub>, the amount of aluminum does not increase linearly with electrolysis duration and it is lower than that expected from the Faraday's law. The corresponding  $\Phi_d$  values, calculated from Eq. (6) for these salts, are reported in Table 1. They are lower than 1 whatever electrolysis duration.

What emerges from these results is that electrolytes may be divided into two categories: those where  $\Phi > 1$  and others where  $\Phi < 1$ . Interestingly, the origin of such differences may be interpreted by invoking the chaotrope/kosmotrope nature of the anions, which is related to ion-specific hydration effects [29,30]. This distinction is conveniently made from the sign of the  $B$  value reported in Table 1, it corresponds to the viscosity coefficient appearing in the Jones-Dole relationship [31]. The value of  $B$  is a direct measure of the strength of ion-water interactions normalized to the strength of the water-water interactions in bulk solution [32]. With kosmotrope (structure-maker) ions, the hydration shell around the ions is thick and it is held strongly (so that the resistance to flow of the aqueous electrolyte solutions is higher than that of pure water). Positive values of  $B$  are thus associated to kosmotrope ions, whereas negative  $B$  values correspond to chaotrope (structure-breaker) ions where the immediately adjacent water molecules are far away and not oriented (the resistance to flow is lower than that of pure water).

Although the influence of anion specificity on the electrochemical

corrosion of anodized (i.e. protected) aluminum alloy substrates has been reported [33], a correlation is evidenced in this study, for the first time to our knowledge, between the faradaic efficiency relative to aluminum oxidation and the specific nature of the anions. So that, for chaotrope anions with  $B < 0$ ,  $\Phi$  is higher than 1 and for kosmotrope anions with  $B > 0$ ,  $\Phi$  is lower than 1. Such a clear distinction reinforces the assumption according to which the categorization of the anions with respect to the value of  $\Phi$  is probably related to the conditions of breakdown of passivity of aluminum by pitting.

Pitting corrosion by aggressive anions occurs at passivated surfaces leading to localized intense dissolution of the underlying metal [34]. The digging of small cavities inside the material, caused by the aqueous phase containing aggressive anions, contributes locally to an appreciable weakening of the metal integrity with irreversible damages, which are responsible of large economic losses and safety problems in metallic constructions [35]. The resistance against corrosion of aluminum, like other valve metals (such as titanium, zirconium, tantalum), is known to result from the existence of a natural and cohesive passive film, with a thickness of few nanometers (about 5 nm typically), when it is exposed to oxidizing media (air, water). In the case of aluminum this surface oxide film (alumina Al<sub>2</sub>O<sub>3</sub>) is stable in the pH range 4–10 in aqueous solution. The reasons why valve metals become irreversibly corroded/pitted depend on the proneness of this passive film to reform (self-healing) sufficiently after its eventual breakdown [36].

The observed distinction according to the specific nature of the anions is assumed to originate from a variable resistance against dehydration when perforating the thin passive film because there exists for the anions a competition between two concomitant effects. Upon voltage application, the anions are attracted towards the anode and they thus come to the passive film-solution interface with their surrounding hydration shell. There, they may be adsorbed onto the passive film and/or may be involved with some surface metallic cations in the formation of more or less soluble salts or complexes, so participating through an eroding process to the thinning of the passive film. However, the chaotrope anions that exhibit a weaker resistance to dehydration can penetrate more easily into the passive film, notably at its defects, up to the metal surface. As a result, they initiate localized corrosion favorably. The restriction of the attack to pits on the large passivated surface should enhance fast oxidation of the metal. During the anodic oxidation and since the number of aluminum atoms released/lost is greater than that expected according to the oxidation reaction, it can be suggested that the attractive forces acting between neighboring aluminum atoms in the created pits were significantly weakened. This may contribute to justify why the faradaic efficiency is systematically higher than 1 in the

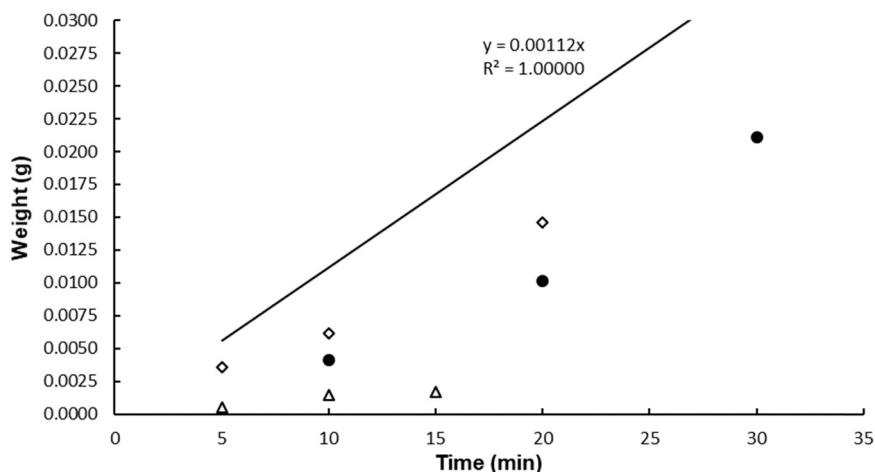


Fig. 2. Weight of aluminum from the ICP dosing method as a function of electrolysis duration in the presence of NaF (◇), Na<sub>2</sub>SO<sub>4</sub> (●) and NaIO<sub>3</sub> (△) at 0.01 mol/L (the continuous line represents Faraday's law).

presence of chaotrope anions.

The aggressiveness of kosmotrope anions is much less pronounced since there exists a marked difference between the hydration state inside the thin passive film (where few water molecules may be entrapped) and outside at the contact of the electrolyte solution where these anions can preserve their hydration state. The energetic dehydration contribution is quite repulsive and it is difficult to overcome. As long as the attractive electric field (voltage) is not sufficiently high to compensate their dehydration (at least partially), the kosmotrope anions remain adsorbed, they are hindered to initiate favorably the pitting process. The latter is absent or it is very limited, so allowing the growth of a thicker alumina oxide film, i.e. anodization, where the prevailing reaction at the anode is in this case:  $2Al + 3 H_2O \rightarrow Al_2O_3 + 6 H^+ + 6 e^-$ . The faradaic efficiency with kosmotrope anions is therefore lower than 1 in such conditions.

The results show the influence of the specific nature of the anions on the faradaic efficiency relative to aluminum oxidation. They indicate that super-faradaic efficiency is observed in the presence of other anions than chlorides, all these anions have a chaotrope nature. This constitutes a novel approach to identify in which conditions the super-faradaic behavior is observed during electrocoagulation with aluminum electrodes. It justifies why supporting electrolytes in electrocoagulation studies should contain a chaotrope anion rather than a kosmotrope anion to allow a favorable release of aluminum cations.

### 3.2. Comparative influence on electrocoagulation efficiency

Depending on the electrogenerated amount of  $Al^{3+}$  cations and the solution pH, consecutive hydrolysis reactions lead to the formation of monomeric hydroxides such as  $Al(OH)^{2+}$ ,  $Al(OH)_2^+$ ,  $Al(OH)_3$ ,  $Al(OH)_4^-$  and also some cationic polymers like  $Al_6(OH)_{15}^{3+}$ ,  $Al_8(OH)_{20}^{4+}$  and  $Al_{13}(OH)_{34}^{5+}$  after sufficient aging [37,38]. For pH values lower than 5,  $Al^{3+}$  cations are the sole ionic species in aqueous phase, they gradually disappear in favor of cationic hydroxides in the pH range 5–7.5. From pH 6, amorphous aluminum trihydroxide  $Al(OH)_3$  precipitates are formed in solution where the highest amount is between pH 6.5 and 7 (solubility is very poor), before they gradually disappear as pH increases to more basic values. Although aluminate anions  $Al(OH)_4^-$  may exist from pH 7, they gradually become the major constituent above pH 8.5 and they are the sole species from pH 10. Thus, the relevance of coagulant species is intimately linked both to the pH level in the system and to the electrical charge of the dispersed entities. The latter depends on the positioning of the iep of the colloidal entity with respect to the solution pH. The charged monomeric hydroxides may be adsorbed onto the surface of dispersed entities (droplets, particles) of opposite charge and/or contribute to an enhanced screening of electrostatic repulsions between the dispersed entities. The increase of ionic strength  $I$  in the system ( $I = \frac{1}{2} \cdot \sum c_{ion} \cdot z_{ion}^2$  where  $c_{ion}$  and  $z_{ion}$  are, respectively, the molar concentration and the number of charges of a given ion in solution) decreases the Debye length  $\kappa^{-1}$ , representing the extent of electrostatic

repulsion between the charged entities, since  $\kappa^{-1} \approx 0.307 \sqrt{I}$  (in nm) in aqueous phase at 25 °C [39]. Within these conditions and as  $I$  is high enough, attractive van der Waals interactions are dominant between the dispersed entities so that aggregation takes place. The resulting aggregates can be enmeshed in the fluffy  $Al(OH)_3$  precipitates in the pH range 6–8.5 through the so-called ‘sweep flocculation’ process [37,40]. In the same time, small electrogenerated hydrogen bubbles coming from water reduction (1) may favor the flotation of aggregates, so allowing an easier removal. When they are present, the cationic polymers can efficiently aggregate several negatively charged particles through bridging flocculation.

#### 3.2.1. Influence of the cation nature on $Al(OH)_3$ precipitates production

It has been shown in previous studies that hydroxyl  $OH^-$  ions, released at the cathode, were not only consumed by electrogenerated

$Al^{3+}$  ions but also by ammonium cations according to the acid-base equilibrium of ammonia (pKa 9.2) associated to its buffering effect [9]:



It seems interesting to investigate whether this may have an influence on the production of  $Al(OH)_3$  precipitates since these species are of utmost importance in particles removal.

Electrolysis of aqueous solutions with aluminum electrodes in the presence of NaCl and  $NH_4Cl$  electrolytes at 0.01 mol/L concentration were carried out at different durations. After electrolysis, the whole volume (100 mL) was poured into glass bottles and the formed  $Al(OH)_3$  precipitates were allowed to settle for some days after gentle manual agitation. The supernatant was then removed as far as possible. The dosing ICP method could not be used to evaluate the aluminum content of the settled precipitates since they were hardly soluble in concentrated nitric acid after a relatively long storage (with ageing the amorphous  $Al(OH)_3$  precipitates evolve into crystalline structures with a whiter aspect). Pure water was added to the settled precipitates in the glass bottles and the resulting suspensions were transferred into centrifuge tubes. Once centrifugation was performed (12,000 rpm during 10 min), the supernatant was rejected and the centrifuge tubes, containing a paste adhering to the wall, were dried in an oven at 50 °C for a week. The amount of solid phase obtained was determined by subtracting the mass of the empty tubes. This method was preferred than centrifugation just after electrolysis to avoid the forced entrainment of soluble species with the fluffy  $Al(OH)_3$  precipitates at the bottom of centrifuge tubes. Photographs of the bottles containing the solutions just after electrolysis are shown in Fig. 3a and b. As it can be seen in Fig. 3a, the amount of settled



Fig. 3. a: Photographs after 5' and 10' of electrolysis in the presence of sodium (Na5' and Na10') and ammonium electrolytes (NH5' and NH10'). Fig. 3b Photographs after 15' and 20' of electrolysis in the presence of sodium (Na15' and Na20') and ammonium electrolytes (NH15' and NH20').

aluminum precipitates after 5' and 10' of electrolysis is greater in the presence of sodium (bottles referred as Na5' and Na10') than with ammonium electrolyte (bottles referred as NH5' and NH10'). This was already obvious during the comparative experiments after 5' of electrolysis. Photographs in Fig. 3b do not exhibit such visual differences between both electrolytes after 15' and 20' of electrolysis (bottles referred as Na15' and Na20' for sodium, bottles referred as NH15' and NH20' for ammonium). As information, the weight loss of the aluminum anode and cathode after 20' of electrolysis was, respectively, 0.0260 g and 0.0019 g, whatever the chloride salt.

As shown in Fig. 4a, the amount of dried aluminum precipitate increases with electrolysis duration in the presence of both electrolytes; it is higher with sodium (black circle) than with ammonium (open square), see the left axis. The mass ratio, defined as the mass obtained with sodium chloride over the mass obtained with ammonium chloride at the same electrolysis duration, is also plotted in Fig. 4a, see the right axis for the values (times symbol). It decreases from 1.70 at 5' to 1.42 at 10' and to 1.09 at 15' before it remains constant, i.e. 1.09 at 20'. This confirms that formation of aluminum precipitates is not favored at the beginning of electrolysis in the presence of ammonium chloride. The corresponding pH variations during electrolysis are reported in Fig. 4b. The initial rise of pH during electrolysis (and electrocoagulation) has been ascribed to the excess cathodic electrogeneration of  $OH^-$  ions with respect to the slower kinetics of  $Al(OH)_3$  precipitates formation [40]. From 5', pH

tends to level off at 7.5 with ammonium electrolyte (open square) whereas it is around 8.5 in the case of sodium electrolyte (black circle).

From the above results, the reported trends in Figs. 3 and 4 may be justified. In the prime instants in the presence of ammonium chloride, the hydroxyl  $OH^-$  ions produced at the cathode are consumed by electrogenerated  $Al^{3+}$  and also by ammonium cations through reaction (7). As such, the rise of pH is more attenuated (see Fig. 4b) and the amount of  $Al(OH)_3$  precipitates is significantly lower with ammonium than with sodium chloride, the corresponding mass ratio is high at 5' (see Fig. 4a). After 10' of electrolysis, pH values are stabilized at 8.5 with sodium and 7.5 with ammonium chloride (see Fig. 4b). The mass ratio decreases (see Fig. 4a) since the increase of the amount of aluminum precipitates is more pronounced with ammonium. Owing to such pH conditions, the proportion of  $Al(OH)_4^-$  anions increases at the expense of  $Al(OH)_3$  precipitates with sodium electrolyte, whereas with ammonium electrolyte the proportion of  $Al(OH)_3$  precipitates increases since it is more favored than cationic aluminum hydroxides and even more than  $Al(OH)_4^-$  anions as pH is 7.5. When electrolysis is prolonged to 15' and over, numerous produced  $OH^-$  ions, even in the presence of ammonium, can react with  $Al^{3+}$  ions to form  $Al(OH)_3$  precipitates. The amount of precipitates is practically the same with both salts, the mass ratio stabilizes near 1 from 15' (see Fig. 4a).

A consequence of these results is that  $Al(OH)_3$  precipitates should not be favored at the beginning of electrocoagulation in the presence of

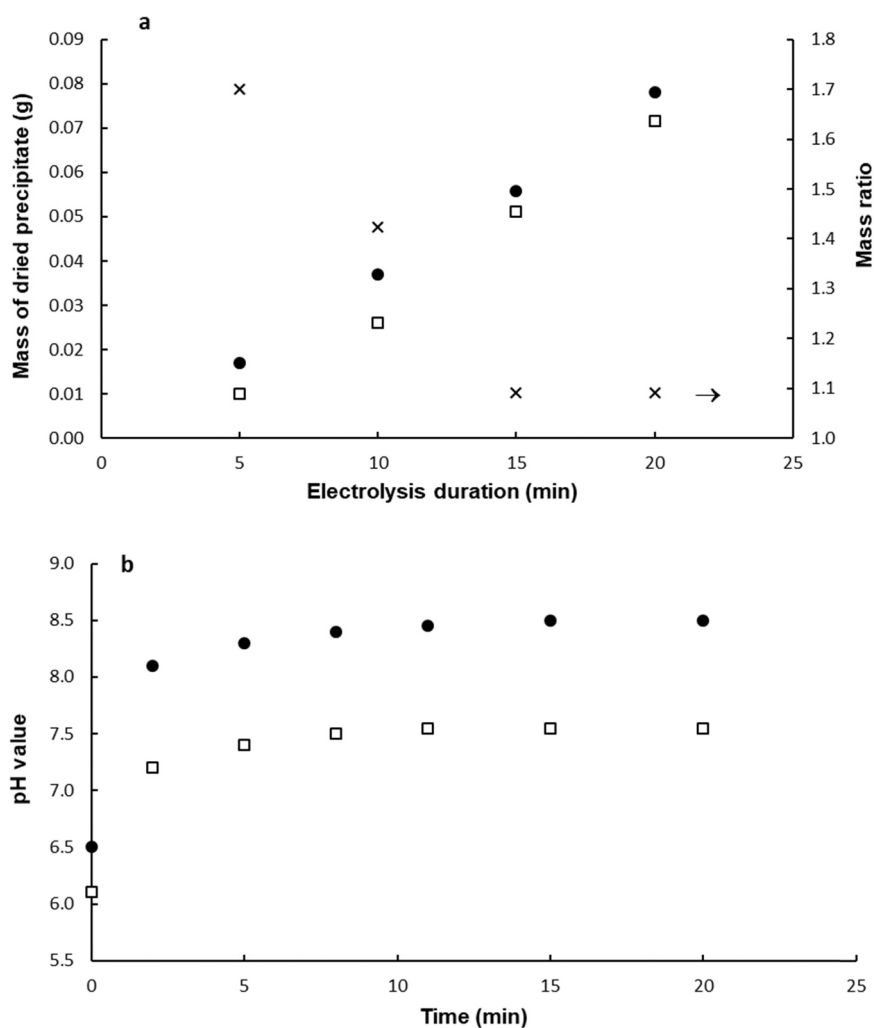


Fig. 4. a. Variation of the mass of dried aluminum precipitate (left axis) with electrolysis duration in the presence of NaCl (●) and NH<sub>4</sub>Cl (□), and variation of the mass ratio (×) at the corresponding electrolysis duration (right axis). Fig. 4b Variation of pH as a function of time during electrolysis with two aluminum plates in the presence of NaCl (●) and NH<sub>4</sub>Cl (□).

ammonium electrolyte. However, provided the initial pH is in the range 6–7, which is often the case, it is expected that the proportion of cationic aluminum hydroxides should increase with respect to  $Al(OH)_3$  since the amount of electrogenerated  $Al^{3+}$  cations is the same whatever the chloride salt for a given electrolysis duration (according to Faraday's law). Therefore, it may be anticipated that in the prime instants with ammonium electrolyte this should have a detrimental effect on the charge screening of positively charged entities and a beneficial effect in the case of negatively charged entities.

### 3.2.2. Influence of the cation nature on the electrocoagulation of negatively charged oil in water emulsion

Semi-skimmed milk is a stable food emulsion composed of fat droplets dispersed in an aqueous phase containing proteins, sugars and salts. The amphiphilic casein proteins with many anionic phosphate groups along the chain act as stabilizing agents for the fat droplets (they represent about 80% of the proteins in bovine milk). In semi-skimmed milk, the content of caseins is nearly the same as in unskimmed milk although the fat content is significantly decreased. As a result, fat globules in semi-skimmed milk are dispersed into smaller droplets than in unskimmed milk. When semi-skimmed milk has been diluted with water at 4% in volume, the size distribution is in the range 80–800 nm with a maximum at 255 nm and a z-average diameter (intensity weighted mean size) corresponding to 235 nm, see Fig. S6 in Supporting Information. The zeta potential of the sample was found to be  $-35$  mV at pH 7 (iep of milk is known to be around 4.5).

Photographs during electrocoagulation experiments of diluted semi-skimmed milk with an imposed 0.200 A electrical intensity in the presence  $NH_4Cl$  and  $NaCl$  at 0.01 mol/L are reported, respectively, in Figs. 5 and in 6. With ammonium salt (Fig. 5), phase separation appears at about 11', see Photograph (a), and it is well amplified at 12', see Photograph (b). After electrolysis and magnetic agitation have been stopped at 13', see Photograph (c), a very clear aqueous phase is observed at 13'30" (white arrows indicate the electrode plates). With sodium salt (Fig. 6), phase separation has not begun at 13'30", see Photograph (a); it is apparent from 15', see Photograph (b). After electrolysis and magnetic agitation have been stopped at 16'30", phase separation is observed at 17', see Photograph (c), although the aqueous phase is still turbid (white arrows indicate the electrode plates), so indicating that electrolysis should be prolonged longer. These results thus confirm the best efficiency of the electrocoagulation treatment in the presence of ammonium.

The origin of such differences is ascribed to the influence of the pH level during electrolysis, as depicted in Fig. 7. Starting from about 7 for both electrolytes, pH rises and it stabilizes after 4' to 8.4 and 9.3, respectively, for ammonium (open square) and sodium (black circle) chloride. The steep pH increase above 9 with sodium electrolyte involves rapidly the enhanced formation of  $Al(OH)_4^-$  anions at the expense of  $Al(OH)_3$  precipitates (the existence of cationic aluminum hydroxides is precluded at this pH level). Such numerous aluminate anions are inefficient to screen the negative charges of the dispersed droplets. They may only participate to the increase of the ionic strength, this contributes to lower the electrostatic repulsions between the droplets. Although the amount of amorphous  $Al(OH)_3$  precipitates is expected to enable the entrapment of the droplets through sweep flocculation, separation is partially effective at 17', see Photograph (c) in Fig. 6. In the presence of ammonium chloride, pH does not increase as much as in the case with sodium electrolyte since the buffer effect takes place owing to reaction (7). As previously indicated in Section 3.2.1, although the formation of  $Al(OH)_3$  precipitates is not favored in the prime instants, the proportion of cationic aluminum hydroxides is promoted so allowing an effective screening of the negative charges of the droplets. From 4' pH remains constant at a level where aluminate anions are formed but it is not excessive with respect to the neutral  $Al(OH)_3$  precipitates. Clear separation is enhanced with ammonium from 13', see Photograph (c) in

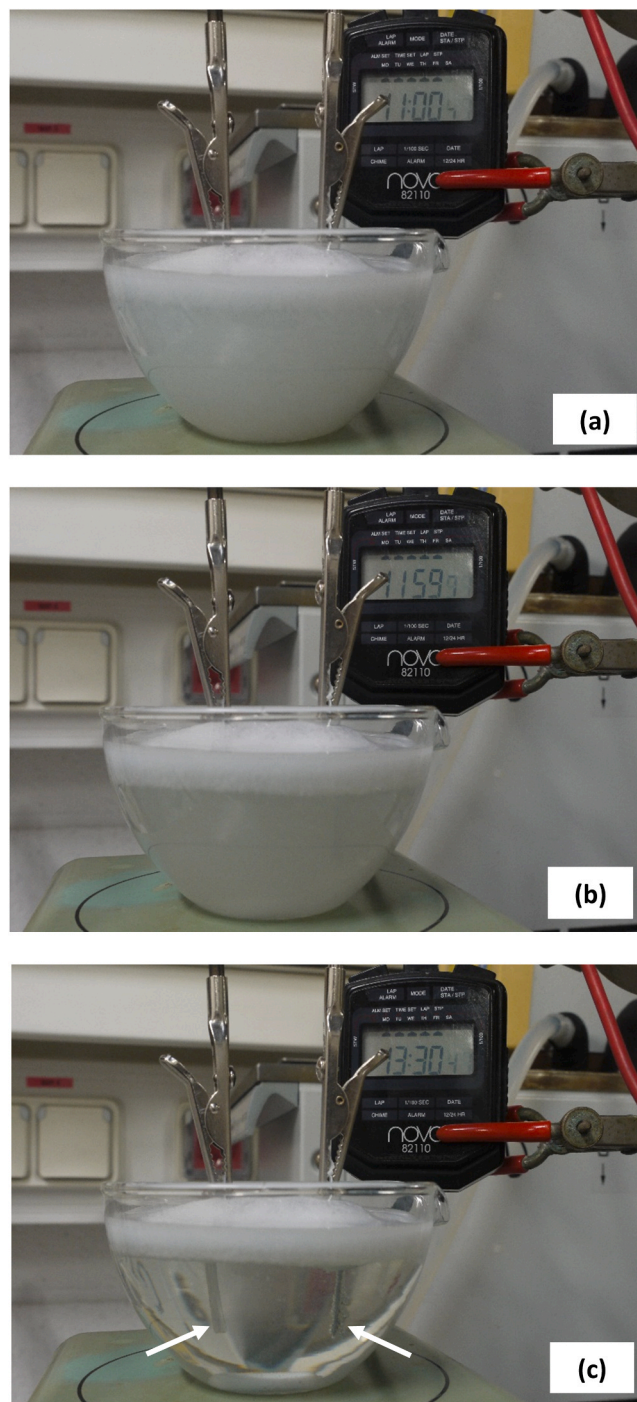


Fig. 5. Photographs during electrocoagulation of diluted semi-skimmed sample in the presence of  $NH_4Cl$  at 11' (a), at 12' (b) and at rest at 13'30" (c).

Fig. 5.

### 3.2.3. Influence of the cation nature on the electrocoagulation of positively charged polystyrene latex

The size distribution of the synthesized latex sample is shown in Fig. S7 in Supporting Information. It is in the range 100–450 nm, with a maximum at 220 nm and a z-average diameter corresponding to 210 nm. A SEM image of the polystyrene latex is presented in Fig. S8 in Supporting Information. The stability of polystyrene particles in solution originates from their electrostatic repulsion due to the positive charges on the particles surface. They result from the 2-methylpropanamide

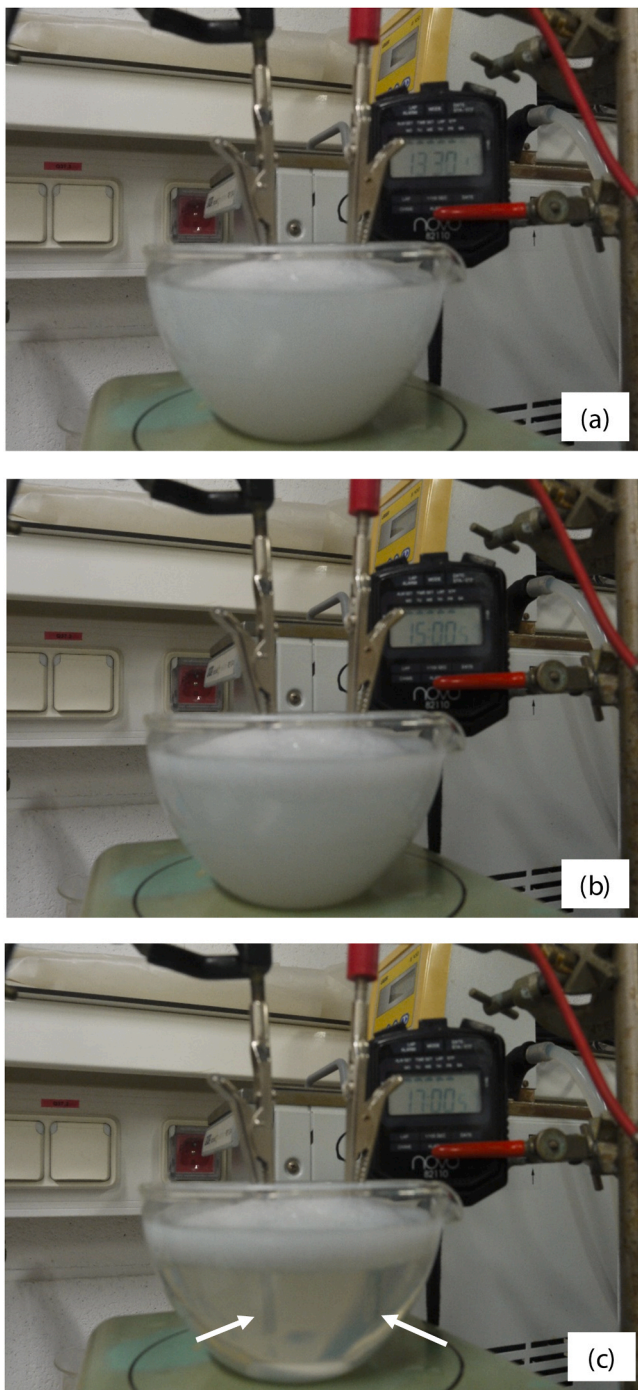


Fig. 6. Photographs during electrocoagulation of diluted semi-skimmed sample in the presence of NaCl at 13'30'' (a), at 15' (b) and at rest at 17' (c).

free radicals  $[(NH_2)_2C-C(CH_3)_2]^{*+}$  generated consecutively to the thermal decomposition of the AIBA initiator through liberation of nitrogen  $N_2$  [14]. In the following step, the radical entity is transferred to styrene monomer. Polymerization reaction then propagates through monomer consumption. The zeta potential of the cationic latex diluted in NaCl solution at 0.001 mol/L was found to be +46 mV. From preliminary tests, the critical coagulation concentration (ccc) of the latex sample was estimated to be around 0.15 mol/L, i.e. the monovalent salt concentration where the particles aggregation regime becomes fast and not reversible [39].

The % COD removal during electrocoagulation of the latex sample with a 0.200 A electrical intensity in the presence of NaCl (black circle)

and  $NH_4Cl$  (open square) at 0.01 mol/L is shown in Fig. 8a. Although the extent of removal is practically the same at the end, separation is faster in this case with sodium chloride. It is achieved at about 25' with ammonium whereas it is only about 15' with sodium salt. The removal of particles increases notably after 5' in both cases although it is significantly higher with sodium salt. The corresponding pH variations, reported in Fig. 8b, are instructive since it is from 5' that pH stabilizes at different levels, i.e. 7.6 and 8.5, respectively, with ammonium (open square) and sodium (black circle) chloride (the initial pH is 6.3 and 6.7, respectively, for ammonium and sodium latex dispersions). In the prime instants of electrocoagulation, cationic aluminum hydroxides such as  $Al(OH)_2^+$  and  $Al(OH)^{2+}$  together with amorphous  $Al(OH)_3$  precipitates are present with both electrolytes (as the initial pH is lower than 7). However, their proportion is expected to decrease rapidly to the benefit of  $Al(OH)_4^-$  formation in the presence of sodium salt since pH reaches 8.5 after 5'. In these conditions, aluminate anions are efficient to screen the positive charges of latex particles, so promoting aggregation. Moreover, the resulting aggregates are collected by the fluffy precipitates through sweep flocculation. This is illustrated by Photograph (a) in Fig. 9 where a clear supernatant is observed when electrocoagulation is stopped at 15' (white arrows indicate the electrode plates).

As expected with ammonium electrolyte, pH levels off at a lower value (see Fig. 8b). At pH 7.5 formation of aluminate anions is not favored, although not precluded, and cationic aluminum hydroxides are present together with fewer  $Al(OH)_3$  precipitates. In these conditions, efficient separation of the positively charged latex particles is difficult. As illustrated by Photograph (b) in Fig. 9 for ammonium electrolyte, the supernatant is still turbid when electrolysis and magnetic agitation are interrupted at 15' while good separation was already achieved with sodium, see Photograph (a). As shown in Fig. 8a and illustrated by Photograph (c) in Fig. 9 (white arrows indicate the electrode plates), suitable separation is delayed up to about 25' with ammonium electrolyte. This occurs when a sufficient amount of aluminum precipitates has been formed, so allowing the entrapment of weakly aggregated latex particles.

The results of this section highlight the detrimental influence of the buffer effect. They justify why separation is so poor with the positively charged latex in the presence of ammonium salt since fewer  $Al(OH)_3$  precipitates are formed from the beginning and a lower proportion of aluminate counterions persists during electrocoagulation. Ammonium electrolytes should be avoided for the electrocoagulation treatment with aluminum electrodes of aqueous effluents containing in majority positively charged entities.

It is noted that with this surfactant-free polystyrene latex, settling of aggregates is observed instead of flotation. Flotation occurs frequently with polymer lattices synthesized from emulsion polymerization because they are stabilized by adsorbed ionic surfactants. Hydrogen bubbles generated at the cathode tend to be collected on the hydrophobic parts of the adsorbed surfactants (similarly as injected air bubbles for ores recovery through froth flotation), so decreasing the apparent density of flocs. As the density of polystyrene is 1.055 g/mL and there is no surfactant, settling of aggregates occurs, i.e. anchoring of hydrogen bubbles is not facilitated.

#### 4. Conclusions

A correlation has been clearly evidenced between the specific nature of the anions and the faradaic efficiency  $\phi$  relative to aluminum oxidation. For chaotrope anions  $\phi > 1$  whereas  $\phi < 1$  for kosmotrope anions. So indicating that this electrochemical parameter, often assessed in electrocoagulation studies with aluminum plates, is dependent on the ability of the anions to lose their hydration shell during the pitting process. The obtained results advocate in this sense.

While the buffering effect imparted by the ammonium electrolyte improves the efficiency of electrocoagulation of negatively charged oil

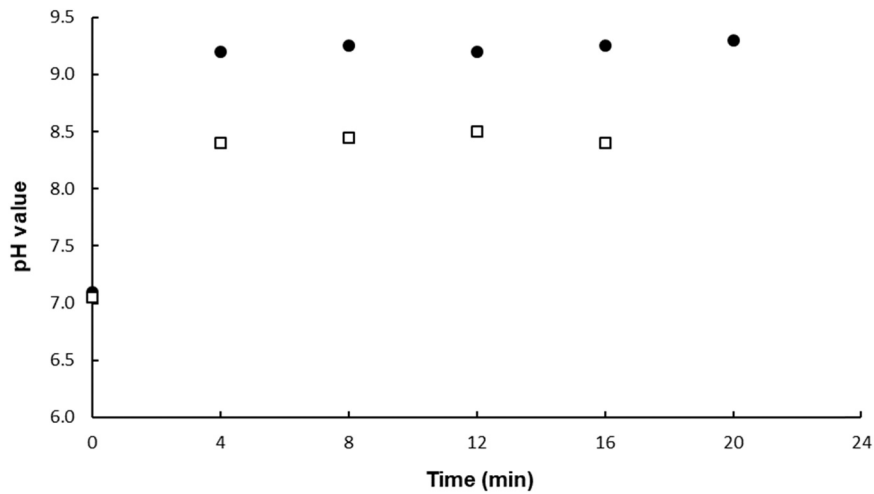


Fig. 7. Variation of pH as a function of time during electrocoagulation of diluted semi-skimmed sample in the presence of NaCl (●) and NH<sub>4</sub>Cl (□).

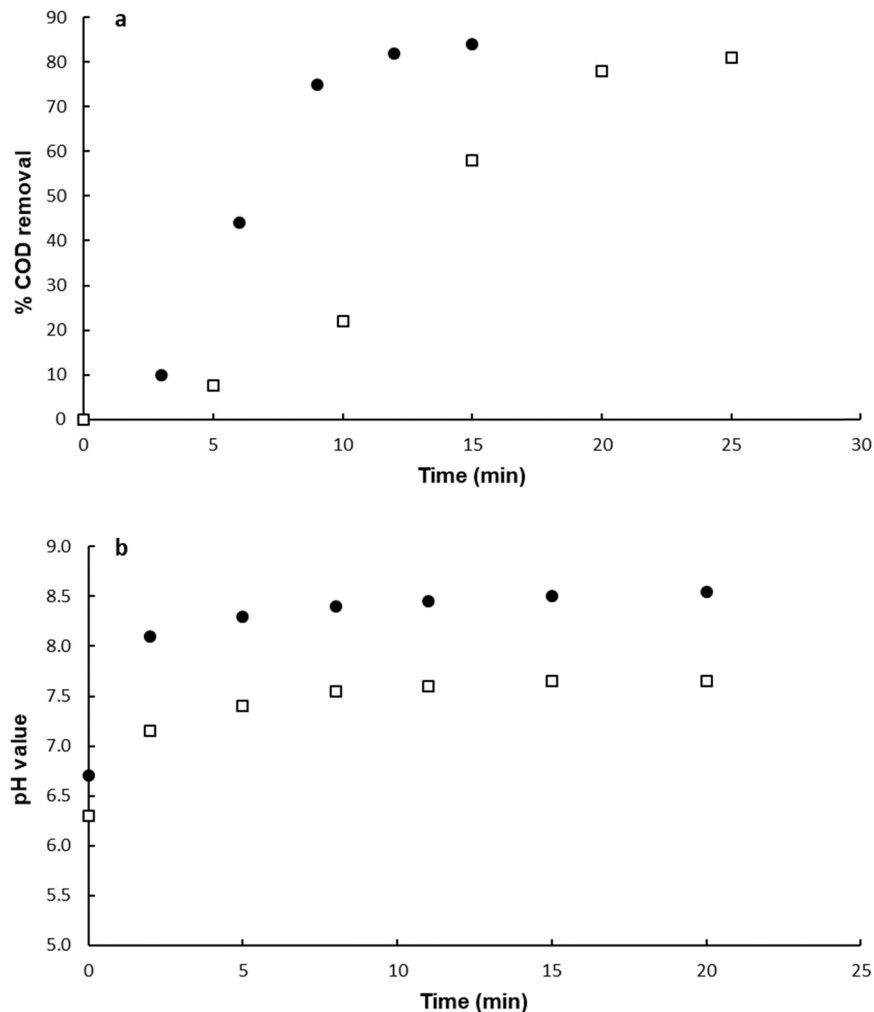


Fig. 8. a: Variation of the % COD removal as a function of time during electrocoagulation of the cationic latex sample in the presence of NaCl (●) and NH<sub>4</sub>Cl (□). Fig. 8b: Variation of pH as a function of time during electrocoagulation of the cationic latex sample in the presence of NaCl (●) and NH<sub>4</sub>Cl (□).

droplets in water, it has a detrimental influence on the treatment of positively charged latex particles when compared to sodium electrolyte. These opposite behaviors emphasize the influence exerted by the nature of the studied cations on the generated aluminum species during electrocoagulation and its consequence on the efficiency of the treatment as

a function of the sign of the charge of the colloidal entities.

#### Funding

This research did not receive any specific grant from funding

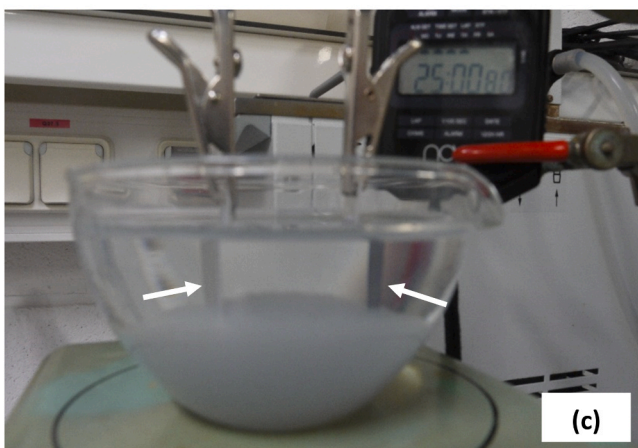
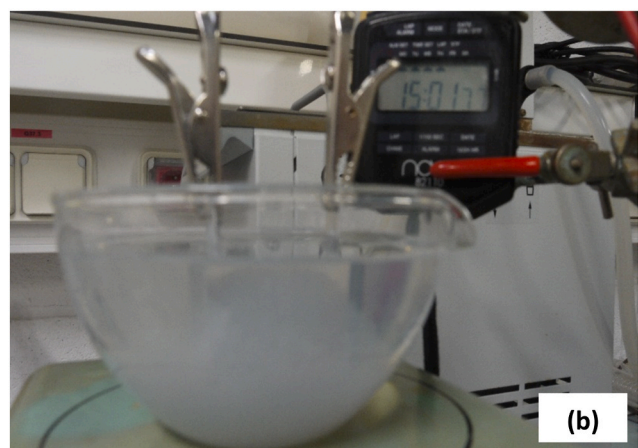
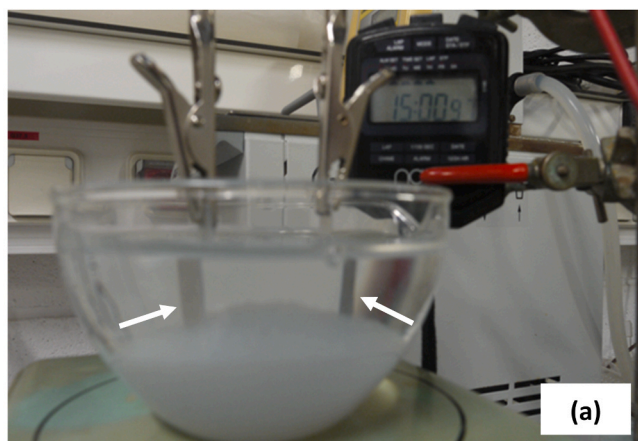


**Fig. 9.** Photographs during electrocoagulation of the latex sample in the presence of NaCl at rest at 15' (a), in the presence of  $\text{NH}_4\text{Cl}$  after interruption at 15' (b) and at rest at 25' (c).

agencies in the public, commercial, or not-for-profit sectors.

#### CRediT authorship contribution statement

**J.L. Trompette:** Conceptualization, Methodology, Validation, Investigation, Writing – original draft, Writing – review & editing, Visualization, **J.F. Lahitte:** Validation, Investigation, Writing – review & editing, Visualization.

#### Declaration of Competing Interest

The authors declare that they have no known competing financial interests or personal relationships that could have appeared to influence the work reported in this paper.

#### Acknowledgments

The authors are grateful to M.L. de Solan-Bethmale, from the LGC, for ICP measurements.

#### Appendix A. Supporting information

Supplementary data associated with this article can be found in the online version at [doi:10.1016/j.colsurfa.2021.127507](https://doi.org/10.1016/j.colsurfa.2021.127507).

#### References

- [1] G. Chen, *Electrochemical technologies in wastewater treatment*, *Sep. Purif. Technol.* 38 (2004) 11–41.
- [2] M.Y.H. Mollah, P. Morkovsky, J.A.G. Gomes, M. Kesmez, J. Parga, D.L. Cocke, Fundamentals, present and future perspectives of electrocoagulation, *J. Hazard. Mater.* B114 (2004) 199–210.
- [3] P.K. Holt, G.W. Burton, C.A. Mitchell, The future for electrocoagulation as a localized water treatment technology, *Chemosphere* 59 (2005) 355–367.
- [4] O. Sahu, B. Mazumdar, P.K. Chaudhari, Treatment of wastewater by electrocoagulation: a review, *Environ. Sci. Pollut. Res.* 21 (2014) 2397–2413.
- [5] S. Garcia-Segura, M.M.S.G. Eiband, J. Vieira de Melo, C.A. Martinez-Huitile, Electrocoagulation and advanced electrocoagulation processes: a general review about the fundamentals, emerging applications and its association with other technologies, *J. Electroanal. Chem.* 801 (2017) 267–299.
- [6] M. Ingelsson, N. Yesri, E.P.L. Roberts, Electrode passivation, faradaic efficiency, and performance enhancement strategies in electrocoagulation - a review, *Water Res.* 187 (2020), 116433.
- [7] I. Gajda, A. Strinchcombe, J. Greenman, C. Melhuish, I. Ieropoulos, Microbial fuel cell - a novel self-powered wastewater electrolyser for electrocoagulation of heavy metal, *Int. J. Hydrog. Energy* 42 (2017) 1813–1819.
- [8] X. Mei, H. Wang, D. Hou, F. Leite Lobo, D. Xing, Z.J. Ren, Shipboard bilge water treatment by electrocoagulation powered by microbial fuel cells, *Front. Environ. Sci. Eng.* 13 (2019) 53.
- [9] J.L. Trompette, H. Vergnes, C. Coufort, Enhanced electrocoagulation efficiency of lyophobic colloids in the presence of ammonium electrolytes, *Colloids Surf. A: Physicochem. Eng. Asp.* 315 (2008) 66–73.
- [10] J.L. Trompette, H. Vergnes, On the crucial influence of some supporting electrolytes during electrocoagulation in the presence of aluminum electrodes, *J. Hazard. Mater.* 163 (2009) 1282–1288.
- [11] P. Canizares, F. Martinez, J. Lobato, M.A. Rodrigo, Break-up of oil-in-water emulsions by electrochemical techniques, *J. Hazard. Mater.* 145 (2007) 233–240.
- [12] C. Jimenez Izquierdo, P. Canizares, M.A. Rodrigo, J.P. Leclerc, G. Valentin, F. Lapique, Effect of the nature of the supporting electrolyte on the treatment of soluble oils by electrocoagulation, *Desalination* 255 (2010) 15–20.
- [13] N.S. Graça, A.M. Ribeiro, A.E. Rodrigues, Removal of fluoride from water by a continuous electrocoagulation process, *Ind. Eng. Chem. Res.* 58 (2019) 5314–5321.
- [14] J.W. Goodwin, R.H. Ottewill, R. Pelton, Studies on the preparation and characterization of monodisperse polystyrene lattices. V: the preparation of cationic lattices, *Colloid Polym. Sci.* 257 (1979) 61–69.
- [15] N. Sharifi-Sanjani, M. Soltan-Dehghan, N. Naderi, A. Ranji, Emulsifier-free emulsion polymerization of styrene, *J. Appl. Polym. Sci.* 94 (2004) 1898–1904.
- [16] T. Picard, G. Cathalifaud-Feuillade, M. Mazet, C. Vandenstendam, Cathodic dissolution in the electrocoagulation process using aluminum electrodes, *J. Environ. Monit.* 2 (2000) 77–80.
- [17] P. Canizares, M. Carmona, J. Lobato, F. Martinez, M.A. Rodrigo, Electrodissolution of aluminum electrodes in electrocoagulation processes, *Ind. Eng. Chem. Res.* 44 (2005) 4178–4185.
- [18] P.K. Holt, G.W. Burton, M. Wark, C.A. Mitchell, A quantitative comparison between chemical dosing and electrocoagulation, *Colloids Surf. A: Physicochem. Eng. Asp.* 211 (2002) 233–248.
- [19] P. Canizares, F. Martinez, C. Jimenez, J. Lobato, M.A. Rodrigo, Comparison of the aluminum speciation in chemical and electrochemical dosing processes, *Ind. Eng. Chem. Res.* 45 (2006) 8749–8756.
- [20] M. Mechelhoff, G.H. Kelsall, N.J.D. Graham, Super-faradaic charge yields for aluminum dissolution in neutral aqueous solutions, *Chem. Eng. Sci.* 95 (2013) 353–359.
- [21] J.Q. Jiang, N.J.D. Graham, C. André, G.H. Kelsall, N. Brandon, Laboratory study of electro-coagulation-flotation for water treatment, *Water Res.* 36 (2002) 4064–4078.
- [22] M. Khemis, J.P. Leclerc, G. Tanguy, G. Valentin, F. Lapique, Treatment of industrial liquid wastes by electrocoagulation: experimental investigations and an overall interpretation model, *Chem. Eng. Sci.* 61 (2006) 3602–3609.

- [23] K. Mansouri, K. Ibrik, N. Bensalah, A. Abdel-Wahab, Anodic dissolution of pure aluminum during electrocoagulation process: influence of supporting electrolyte, initial pH, and current density, *Ind. Eng. Chem. Res.* 50 (2011) 13362–13372.
- [24] E. Fekete, B. Lengyel, T. Cserfalvi, T. Pajkossy, Electrochemical dissolution of aluminum in electrocoagulation experiments, *J. Solid State Electrochem* 20 (2016) 3107–3114.
- [25] G. Mouedhen, M. Feki, M. De Petris Wery, H.F. Ayedi, Behavior of aluminum electrodes in electrocoagulation process, *J. Hazard. Mater.* 150 (2008) 124–135.
- [26] K. Bensadok, F. Bennamar, F. Lapique, G. Nezzal, Electrocoagulation of cutting oil emulsions using aluminum plate electrodes, *J. Hazard. Mater.* 152 (2008) 423–430.
- [27] M. Mechelhoff, G.H. Kelsall, N.J.D. Graham, Electrochemical behavior of aluminum in electrocoagulation processes, *Chem. Eng. Sci.* 95 (2013) 301–312.
- [28] D.M. Drazic, J.P. Popic, Anomalous dissolution of metals and chemical corrosion, *J. Serb. Chem. Soc.* 70 (2005) 489–511.
- [29] W. Kunz, Specific ion effects in colloidal and biological systems, *Curr. Opin. Colloid Interface Sci.* 15 (2010) 34–39.
- [30] A. Salis, B.W. Ninham, Models and mechanisms of Hofmeister effects in electrolyte solutions, and colloid and protein systems revisited, *Chem. Soc. Rev.* 43 (2014) 7358–7377.
- [31] H.D.B. Jenkins, Y. Marcus, Viscosity B-coefficients of ions in solution, *Chem. Rev.* 95 (1995) 2695–2724.
- [32] K.D. Collins, Ions from the Hofmeister series and osmolytes: effects on proteins in solution and in the crystallization process, *Methods* 34 (2004) 300–311.
- [33] J.L. Trompette, L. Arurault, S. Fontorbes, L. Massot, Influence of the anion specificity on the electrochemical corrosion of anodized aluminum substrates, *Electrochim. Acta* 55 (2010) 2901–2910.
- [34] G.S. Frankel, Pitting corrosion of metals, *J. Electrochem. Soc.* 145 (1998) 2186–2198.
- [35] H.H. Strehblow, Mechanisms of pitting corrosion, in: P. Marcus (Ed.), *Corrosion Mechanisms in Theory and Practice*, Second ed., Marcel Dekker, Inc, New York, 2002, pp. 243–286 (Chapter 8).
- [36] H.S. Isaacs, The localized breakdown and repair of passive surfaces during pitting, *Corros. Sci.* 2 (1989) 313–323.
- [37] J. Duan, J. Gregory, Coagulation by hydrolyzing metal salts, *Adv. Colloid Interface Sci.* 100–102 (2003) 475–502.
- [38] C. Hu, S. Wang, J. Sun, H. Liu, J. Qu, An effective method for improving electrocoagulation process: optimization of  $Al_{13}$  polymer formation, *Colloids Surf. A: Physicochem. Eng. Asp.* 489 (2016) 234–240.
- [39] P.C. Hiemenz, *Principles of Colloid and Surface Chemistry*, second ed., Marcel Dekker, New York, 1986.
- [40] T. Harif, M. Khai, A. Adin, Electrocoagulation versus chemical coagulation: coagulation/flocculation mechanisms and resulting flocculation characteristics, *Water Res.* 46 (2012) 3177–3188.